



SEISMIC PERFORMANCE OF US STEEL BOX COLUMN CONNECTIONS

Taejin KIM¹, Bozidar STOJADINOVIC² and Andrew S. WHITTAKER³

SUMMARY

The FEMA connections are prequalified only for steel moment connections to US W-shape columns. Built-up box columns with inner diaphragm plates are often used in US, but there are no test data upon which to base a performance evaluation or develop retrofit solutions for the connection to typical box columns. The objective of this paper is to investigate the seismic performance of steel moment connections to US box columns fabricated using pre-Northridge connection details. Two full-scale cyclic tests were conducted for the steel moment connections, one between ASTM A572 Grade 50 W33×118 beam and BC18×18×257 built-up box column, and one between ASTM A572 Grade 50 W36×232 beam and BC31.5×13×464 built-up box column. Both test specimens failed by brittle fracture of the CJP welds between the beam flange and the column. Solid element models for each test specimens were made and analyzed to investigate the stress and strain states at the critical section of the joint between a W-shape beam and a box-shape column. The stress and strain distributions across the width of the beam flange near the column were affected by out-of-plane stiffness of the column flange plate. As the stiffness increased, the axial strain distribution became uniform. Local yielding of the beam flange may delay the brittle crack propagation in the CJP welds. Careful detailing and using the notch-tough weld metal are required to join the continuity plates and column plates.

INTRODUCTION

Practical design guidelines, published in a series of FEMA documents, gave designers new tools to design special steel moment frames and provided a portfolio of new connection solutions. Satisfactory seismic behavior of the new connections was proven in a comprehensive series of pre-qualification tests. Such tests are now mandatory for every new connection that falls outside the parameter space tested to date (FEMA [1]). FEMA connections are prequalified only for US W-shape columns, but box-shaped columns were not considered. There is not enough test data upon which to base a performance evaluation or develop retrofit solutions for the connection to typical box columns. Built-up columns are often used in US, because they can be made stronger than cold formed tubes. Continuity plates (inner diaphragms) are usually installed inside the box at the levels of both beam flanges.

¹ Assistant Professor, SungKyunKwan University, Suwon, Korea. Email: taejin@skku.edu

² Associate Professor, University of California, Berkeley, USA. Email: boza@ce.berkeley.edu

³ Associate Professor, University of Buffalo, USA, Email: awhittak@acsu.buffalo.edu

The objective of this study is to investigate the seismic performance of welded steel moment connections to US box columns. Two full-scale tests of steel moment connections between W-shape beams and built-up box columns were conducted under cyclic loading. Solid element models representing both test specimens were prepared and response analyses were conducted under monotonic loading. This paper summarizes the key findings of these studies.

EXPERIMENTAL PROGRAM

Test Specimen Design and Fabrication

The test specimens were designed using as-built construction data from a building constructed before 1994 Northridge earthquake (Kim [2]). The column height of each specimen was selected to match the typical story height in the building (4.166 m). The lengths of the beams were set equal to half of the span of the corresponding beam in the building, subject to a maximum span of 8.23 m (27 feet). This limitation (producing a maximum beam length from the centerline of the column to the centerline of the actuator of 4.114 m) was set because the maximum stroke of the actuator was 508 mm: accepting a longer beam span would have limited the drift angle that could be imposed on the test specimens. Summary information on each specimen is presented in Table 1. Figure 1 presents the connection details for Specimens EC01 and EC02.

The continuity plates, W-shape beams, and box columns were fabricated from ASTM A572 Grade 50 steel; shear tabs were fabricated from ASTM A36 steel. Lincoln E70T-4 filler metal was specified for all complete joint penetration (CJP) beam-to-column welds in the test connections. Coupons were extracted from the four W-shapes (W33×118 and W36×232) from remnants of the sections following fabrication. Two tensile samples were taken from the flange sections and two tensile samples were taken from the web sections of each wide flange beam. Steel coupon tests were conducted in accordance with ASTM A370. Average values of yield and tensile strength from the coupon tests are summarized in Table 2. Mill test report (MTR) data for the components of the specimens are also summarized in this table.

Table 1. Dimensions of test specimens

	Specimen EC01	Specimen EC02
Beam length (mm) ¹	2,286	4,114
Beam size	W33×118	W36×232
Shear tab thickness (mm)	16	16
Fillet weld on shear tab (mm)	11	0
Column height (mm)	4,166	4,166
Column size	BC18×18×257	BC31.5×13×464
Box column plate thickness (mm)	29	70 (flange), 32 (web)
Continuity plate thickness (mm)	25	25
Number of bolts in shear tab ³	9	9

1. Distance from column centerline to actuator centerline, 2. NA = Not applicable.

3. A490SC bolts, diameter = 29 mm.

Table 2. Mechanical properties for the W-shape beams

Member	Location	Yield strength (MPa)		Tensile strength (MPa)	
		MTR ¹	Coupon	MTR ¹	Coupon
W33×118	Flange	418	426	525	527
	Web	418	479	525	549
W36×232	Flange	392	374	520	521
	Web	392	422	520	522

1. MTR= mill test report.

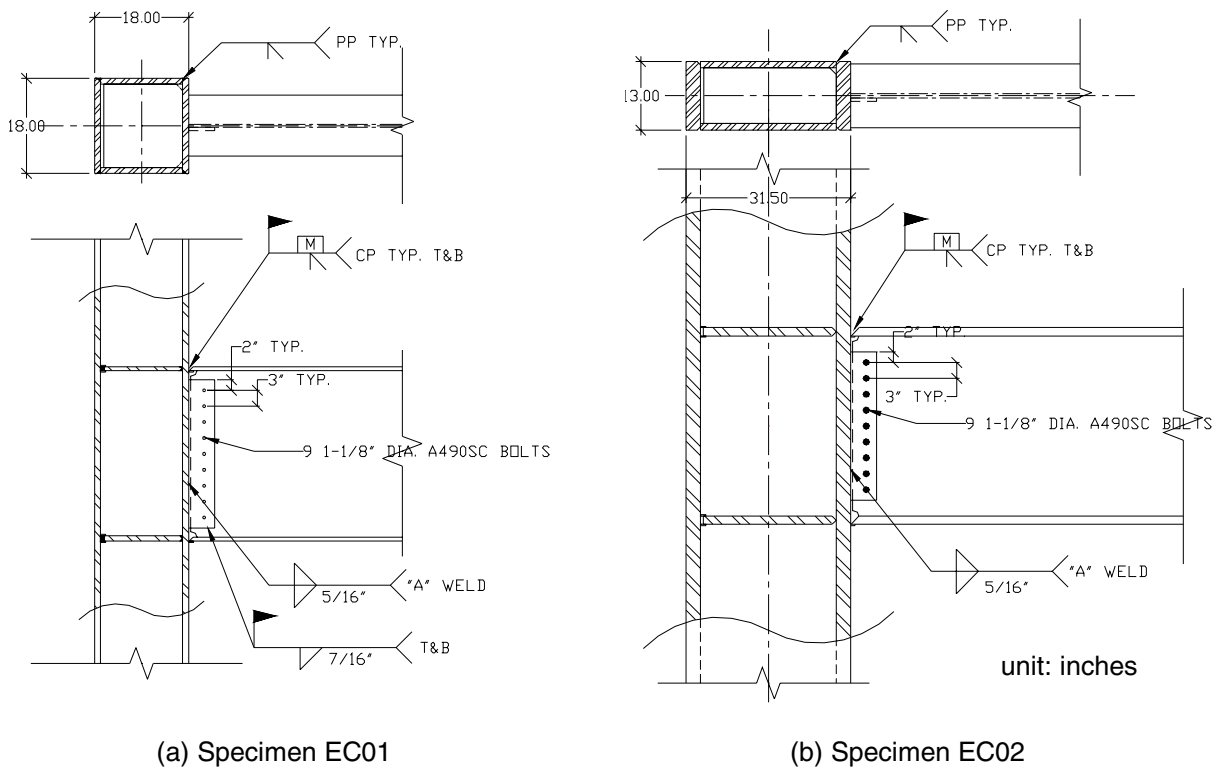


Figure 1. Connection details between W-shape beams and box columns

Test Setup and Loading Protocol

Figure 2 shows a plan view of the test fixture for Specimen EC02. This fixture was designed to accommodate all specimens in horizontal plane, 577 mm above the strong floor. The columns were anchored at each end with machined pinned connections developed for a previous connection-testing project (Whittaker [3]). These pins were installed in large-size clevises attached to steel reaction blocks that were welded to 31 mm thick steel plates placed on the strong floor. The reaction plates were stressed to the strong floor. The free end of the beam was attached to two 2224-kN, 508-mm stroke actuators installed in the custom-made reaction boxes. These reaction boxes were also stressed to the strong floor.

The test fixture included two lateral-restraint frames that served to replicate the restraint conditions in the field. The lateral-restraint frames were designed to resist over 10 percent of the maximum expected axial strength of the beam flange among the test specimens. HSS 5×5×1/4" tube was used for the lateral-restraint frame near the actuator and HSS 6×6×5/8" tube was used for the lateral-restraint frame in the middle of the beam. Only one lateral-restraint frame near the actuators was used for Specimen EC01.

The instrumentation for the test specimens consisted of: two load cells in-line with the actuator measuring axial force; an NVTC (Novotechnic linear potentiometer) at the beam end measuring the imposed displacement; uniaxial and rosette strain gages to measure local strains; displacement transducers placed on the panel zone and column measuring deformations; displacement transducers placed on the bottom of column measuring the twist of the column; displacement transducers on the beam flange measuring the amplitude of flange local buckling; uniaxial and rosette strain gages measuring the brace force; displacement transducers placed on the strong floor measuring the reaction frame slip; and displacement transducers placed on the clevis measuring the gap and slip between the clevis plate and column end plate.

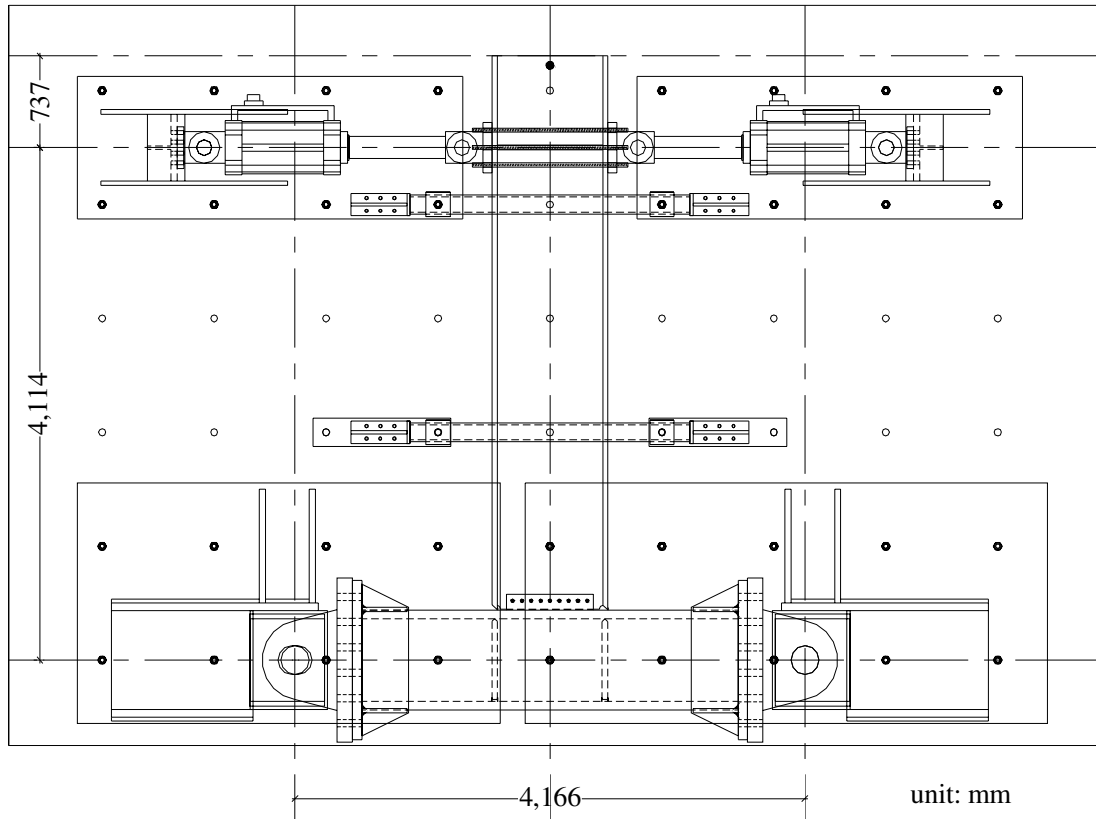


Figure 2. Plan view of test setup for Specimen EC02

Symmetric and stepwise-increasing displacements (SAC [4]) were imposed on the beam by the actuators at the end of the beam. Story drift was used as the control variable. The complete displacement history consisted of thirty-four cycles; six cycles at a target drift angle of 0.375-percent, 0.500-percent, and 0.750-percent, four cycles at a target drift angle of 1.0-percent, and two cycles at a target drift angles of 1.5-percent, 2.0-percent, 3.0-percent, 4.0-percent, and 5.0-percent. Testing using this displacement history continued until the beam completely separated from the column.

EXPERIMENTAL RESULTS

Global Responses

Global response data in the form of moment-story drift angle relations are presented. Moment-beam plastic rotations are not plotted because the specimens fractured before specimen yielding. The reference moment presented for each specimen is the moment at the face of the column, which was calculated by multiplying the actuator force by the distance between the centerline of the actuator and the face of the column. Story drift angle was computed by dividing the beam tip displacement by the distance between the displacement measuring point and the centerline of the column. The relations between moment (at the column face) and story drift angle for Specimens EC01 and EC02 are presented in Figure 3 and Figure 4, respectively.

Summary data from the tests of the two specimens are tabulated in Table 3: a) the plastic moment of the beam section based on the nominal yield strength of 345 MPa (50 ksi); b) the plastic moment of the beam section based on the yield strength calculated from mill test reports; c) the maximum beam moment at the column face prior to fracture normalized by the plastic moments of (a) and (b); d) the story drift angle at first beam flange fracture; e) the maximum beam plastic rotation; f) the maximum panel zone plastic

rotation; g) the maximum beam moment following the fracture of both beam flanges normalized by the plastic moment of (a); and h) the story drift angle at fracture or failure of the web tab.

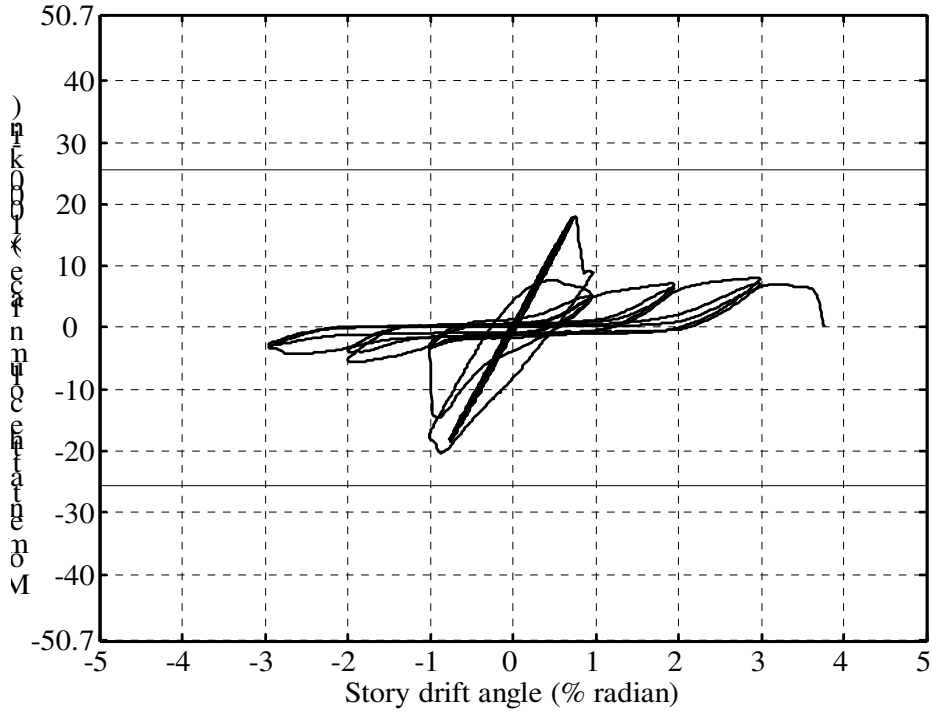


Figure 3. Moment-drift response of Specimen EC01

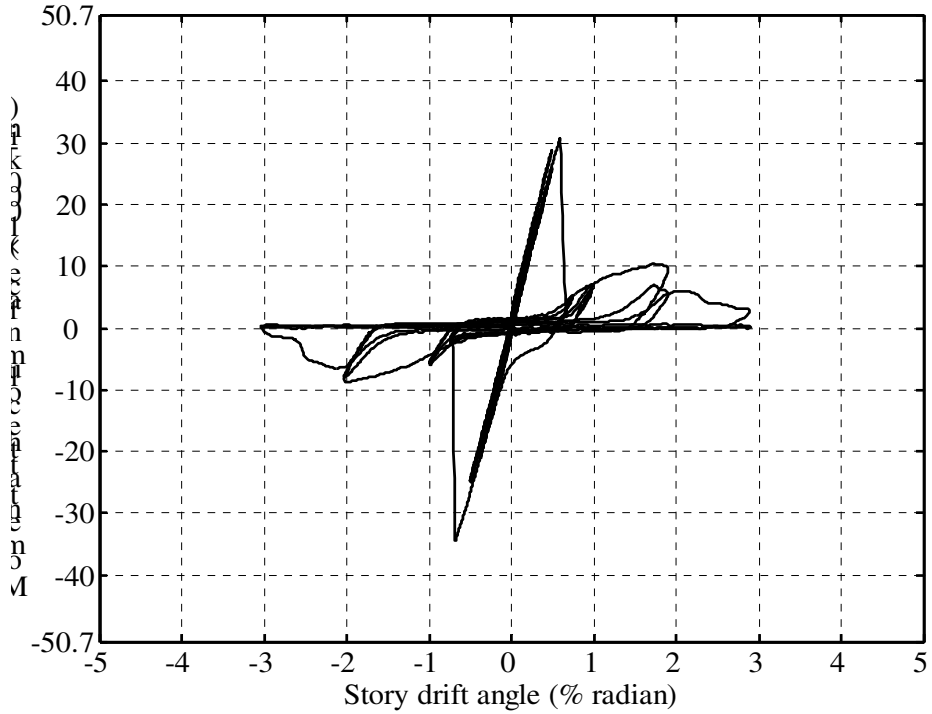


Figure 4. Moment-drift response of Specimen EC02

Table 3. Response Summary

	$M_p = ZF_y$ kN·m	$M_p^* = Z\sigma_y$ kN·m	M_{max} / M_p	M_{max}^* / M_p^*	$\theta_{fr,flg}$ rad.	$\theta_{p,b}$ rad.	$\theta_{p,pz}$ rad.	M_{fr} / M_p	$\theta_{fr,web}$ rad.
EC01	2,344	2,860	0.86	0.71	0.0078	0	0	0.42	0.04
EC02	5,288	6,028	0.66	0.58	0.0059	0	0	0.22	0.03

Specimen EC01

Yielding of the top and bottom flanges of the beam was observed during the first displacement excursion to a drift angle of 0.75-percent. Three cracks in the CJP weld of the beam top flange to the column flange formed just prior to fracture of the top flange. Figure 5a shows the locations of these three cracks. They propagated rapidly following initiation, (this took approximately 0.03 seconds, measured by video image data recorded during the test), and joined, leading to top flange fracture. The beam top flange of Specimen EC01 fractured at the story drift angle of 0.78-percent during the first displacement excursion to a story drift angle of 1-percent. Figure 5b is a photograph of the fractured top flange. Fracture of the top flange was followed by fracture of the supplemental fillet weld to the web shear tab: see Figure 6a. The beam bottom flange fractured at a story drift angle of 0.91-percent during the second displacement excursion to a story drift angle of 1-percent. Following fracture of the beam bottom flange, a tear developed in the shear tab. This tear propagated slowly in subsequent cycles. The test was terminated when the shear tab fractured along a line through the bolts during the first excursion to a story drift angle of 4-percent.



(a) Cracks in CJP weld

(b) Fracture pattern

Figure 5. Crack propagation during beam top flange fracture of Specimen EC01

The positive (tension in the top flange and compression in bottom flange) maximum moment at the column face before the first fracture was 2,026 kN-m (17,934 kip-in), which is 86 percent of the plastic moment based on the nominal yield strength of 345 MPa (50 ksi) or 71 percent of the plastic moment based on the MTR yield strength of 418 MPa (61 ksi). The negative (compression in the top flange and tension in the bottom flange) peak moment before the bottom flange fractured was 2,294 kN-m (20,300 kips-in), which is 98 percent of the plastic moment based on the nominal yield strength of 345 MPa (50 ksi) or 81 percent of the plastic moment based on the MTR yield strength of 418 MPa (61 ksi).

The peak moment resisted by the shear tab after both flanges had fractured was 995 kN-m (8,804 kip-in), which is 42 percent of the plastic moment of the connection based on the nominal yield strength, and 3 times larger than the plastic moment of the shear tab alone based on a nominal yield strength for the tab steel of 248 MPa (36 ksi). This large residual strength is developed by the couple between the

compressive force transferred across the fractured beam flange and a resultant tensile force carried by the bolts of the shear tab.



(a) Fillet weld fracture in Specimen EC01

(b) Shear tab tearing in Specimen EC02

Figure 6. Initiation of shear tab failures

Specimen EC02

Yielding of the bottom flange of the beam was observed during the first displacement excursion to a drift angle of 0.375-percent. Yielding of the beam top flange was not observed prior to top flange fracture. The beam top flange of Specimen EC02 fractured at the story drift angle of 0.59-percent during the first displacement excursion to a story drift angle of 0.75-percent (see Figure 7). The beam bottom flange fractured at a story drift angle of 0.68-percent during the following negative displacement excursion to a story drift angle of 0.75-percent. A tear developed in the shear tab, as shown in Figure 6b, during the displacement excursions to a story drift angle of 2-percent. This tear propagated slowly in subsequent cycles. The test was terminated when the shear tab fractured along a line through the bolts during the first excursion to a story drift angle of 3-percent.



(a) CJP weld before fracture

(b) Fracture pattern

Figure 7. Beam top flange fracture of Specimen EC02

The positive (tension in the top flange and compression in bottom flange) maximum moment at the column face before the first fracture was 3,473 kN-m (30,736 kip-in), which is 66 percent of the plastic

moment based on the nominal yield strength of 345 MPa (50 ksi) or 58 percent of the plastic moment based on the MTR yield strength of 393 MPa (57 ksi). The negative (compression in the top flange and tension in the bottom flange) peak moment before the bottom flange fractured was 3,897 kN-m (34,489 kip-in), which is 74 percent of the plastic moment based on the nominal yield strength of 345 MPa (50 ksi) or 65 percent of the plastic moment based on the MTR yield strength of 393 MPa (57 ksi).

The peak moment resisted by the shear tab after both flanges had fractured was 1,173 kN-m (10,382 kip-in), which is 22 percent of the plastic moment of the connection based on the nominal yield strength, and 3.5 times larger than the plastic moment of the shear tab alone based on a nominal yield strength for the tab steel of 248 MPa (36 ksi).

Local Responses

Local responses in the beam and column flanges and webs are reported in terms of strains. In the following presentations, the strains are normalized with respect to an assumed yield strain of 0.002. The normalized strain for each drift cycle is computed when the force attains its peak.

Figure 8 shows the maximum tensile strain profiles on the beam top flange of Specimens EC01 and EC02 during the each drift cycle. This strain distribution was recorded by strain gages attached on the top surface of the top flange along a line at a distance of 51 mm (2 in.) from the column face during the positive loading half-cycle (producing tension in the top flange). The strain was normalized by an assumed yield strain of 0.002, typical for Grade 50 steel. The strains were highest at the edges of the beam flange and lowest in the middle of the beam flange above the web. This result was expected because there is no column web in the box column to provide restraint for the beam flange. Instead, such restraint is provided by the box column side plates and affects the edges of the beam flange. The strain distribution across the width of the beam flange of Specimen EC02 was more uniform than that for EC01 because the out-of-plane bending stiffness of the column flange plate was much higher in EC02: the thickness of the EC02 flange plate was 70 mm, compared to 29 mm for EC01, while the width of the EC02 flange was 330 mm, compared to 457 mm for EC01.

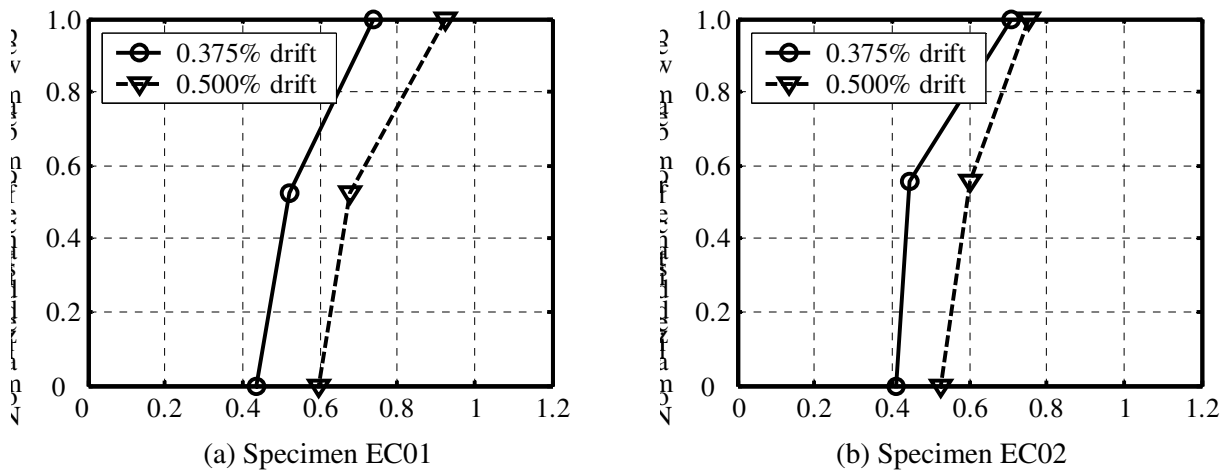


Figure 8. Normalized peak tensile strain profiles on Beam top flanges (ϵ/ϵ_y)

ANALYTICAL INVESTIGATION

Numerical Models

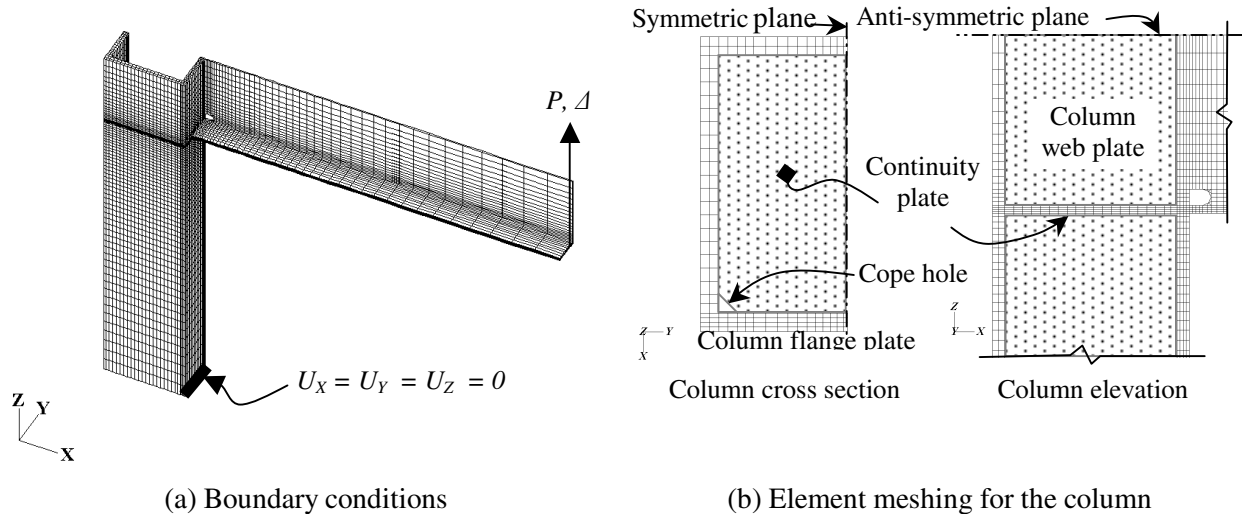
Version 6.3 of ABAQUS (HKS [5]) was used in the analytical investigation. Solid element models were prepared for each test specimen. The beam, column, and plates in these connections were discretized using three-dimensional solid elements. These solid models were used to study the stress and strain distributions in the connections at different levels of story drift. However, the solid models were not used

to capture local and global instabilities such as flange- and web-local buckling, and lateral-torsional buckling (Kim [6]).

The coordination system, finite element meshes and boundary conditions of the solid element models for Specimen EC01 are presented in Figure 9a. The global coordinate system (X, Y, Z) was used as the reference frame for each local coordination system, loading, and boundary conditions. The X -direction coincides with the longitudinal axis of the beam; the Z -direction coincides with the longitudinal axis of the column. The out-of-plane Y -direction is defined by the right-hand screw rule.

To reduce the computational effort, only one quarter of each specimen was modeled, taking advantage of symmetry and asymmetry in the model. These models take advantage of symmetry about the Z - X plane ($y=0$) and anti-symmetry about the X - Y plane of the specimen. In the quarter model, only half of the height and width of the column and half of the depth and width of the beam were modeled.

The *symmetric* boundary condition about the Z - X plane (*YSYMM* in ABAQUS) constrains the displacement along the Y -axis and rotations (first derivative of the displacement) about the Z - and X -axes to be zero. The *anti-symmetric* boundary condition about the X - Y plane (*ZASYMM* in ABAQUS) constrains the displacements along the X -axis and Y -axis and rotations about the Z -axis to be zero. Figure 9b shows element meshes for the quarter model of Specimen EC01 in the (X, Y, Z) coordinate system.



(a) Boundary conditions

(b) Element meshing for the column

Figure 9. ABAQUS Solid model of Specimen EC01 (SOL-EC01)

Local Responses at Fracture

The sizes of members and lengths of beams in Specimens EC01 and EC02 differed. Thus, stress and strain states in these specimens at a given drift may not be the same making it difficult to do a comparison. For the purpose of comparison between two specimens, story drift angles at the first brittle fracture of each specimen are selected as the reference points. The fracture drift of Specimen EC01 was 0.78-percent radian and that of Specimen EC02 was 0.59-percent radian.

Figure 10 shows the contours of maximum principal stresses and equivalent plastic strains on the interface between the beam flange and the column flange of Specimen EC01, at the story drift of 0.78-percent. The maximum principal stresses were normalized using the yield stress obtained from the coupon test. The normalized maximum principal stress is 1.53 (corresponding to 654 MPa or 94.8 ksi) at Point A, 1.48 (629 MPa or 91.2 ksi) at Point B, and 1.44 (614 MPa or 89.0 ksi) at Point C. The equivalent plastic strain is 0.003 at Point A and 0.0054 at Point C. The equivalent plastic strain in the beam flange edge (near Point B) ranges from 0.002 to 0.005, showing moderate yielding. The high values of the maximum principal stress at the extreme fiber of the beam flange caused the cracks that had been developed before fracture: see Figure 5a. Because both edges of the beam flange yield while the center region of the beam flange is still elastic at the story drift of 0.78-percent radian, the cracks in both edges of the beam flange

propagate in a ductile manner (slow crack growth; Stojadinovic [7]) while the crack in the beam flange center propagates in brittle fashion (rapid crack growth without any energy dissipation).

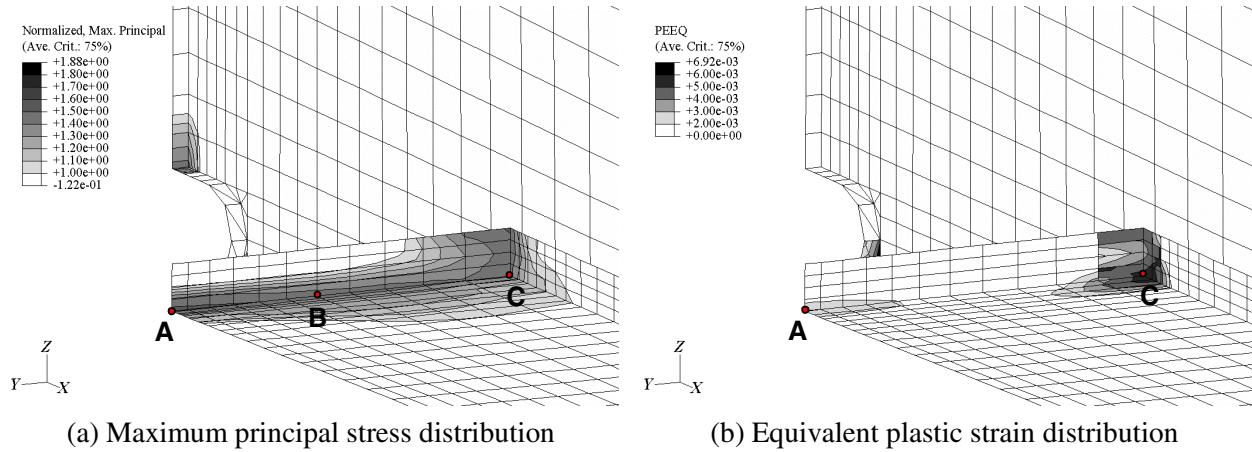


Figure 10. Responses on the interface of the beam flange in Model SOL-EC01 at 0.78-percent drift

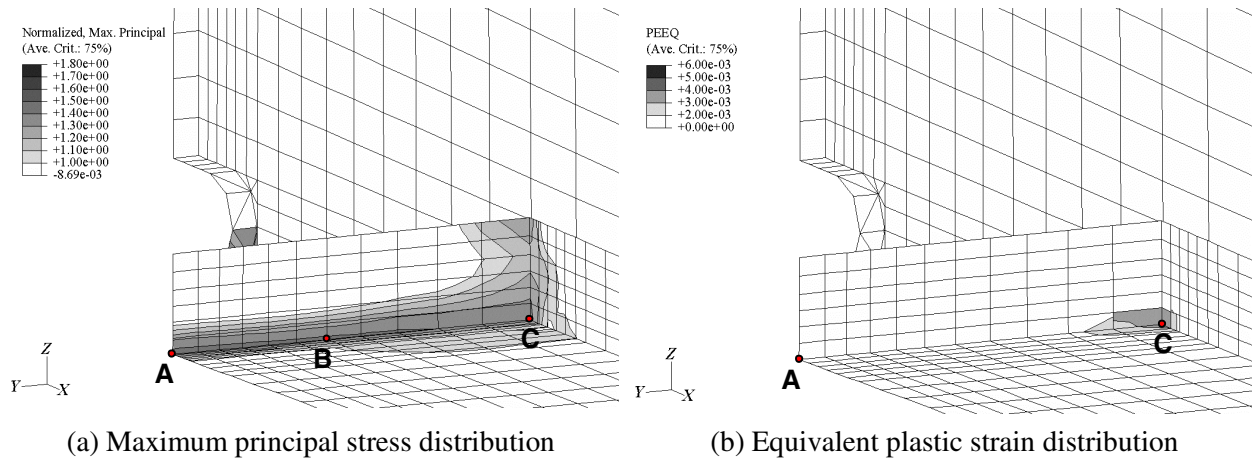


Figure 11. Responses on the interface of the beam flange in Model SOL-EC02 at 0.59-percent drift

Figure 11 shows the contours of normalized maximum principal stresses and equivalent plastic strains on the interface between the beam flange and the column flange of Specimen EC02, at the story drift of 0.59-percent. The normalized maximum principal stress is 1.46 (corresponding to 546 MPa or 79.2 ksi) at Point A, 1.43 (535 MPa or 77.6 ksi) at Point B, and 1.36 (507 MPa or 73.6 ksi) at Point C. The equivalent plastic strain is 0.001 at Point A and 0.0034 at Point C. The area of equivalent plastic strains greater than 0.002 in Model SOL-EC02 is much smaller than those in Model SOL-EC01 while the magnitudes of normalized maximum principal stresses in each model are similar. Thus cracks developed at the edges of the beam flange of Specimen EC02 propagate rapidly. The cracks could not be observed during the test because the interval from nucleation to crack propagation was so short and the video image recorded at 33 frames per second was not sufficiently fast to record brittle crack propagation. The maximum principal stress at the expected crack location of Specimen EC02 is lower than that of Specimen EC01. Because the same weld metal was used for both specimens, the level of the maximum principal stress might be the same to develop microcracking (Kim [2]). If the variance in material properties of both welds is small, the difference of the maximum principal stress at fracture can be explained by the residual stress caused by welding process (Zhang [8]). Because the volume of weld metal for CJP weld in the Specimen EC02 is much larger than that in Specimen EC01, higher residual stresses could exist in CJP welds of Specimen

EC02. Such residual stress may elevate the level of actual maximum principal stress in Specimen EC02 compared to that in Specimen EC01.

CJP Welds of Continuity Plates

The box columns of Specimens EC01 and EC02 are built-up sections, which are fabricated by welding the component plates. Partial joint penetration (PJP) welds were used to join the column plates. Interior continuity plates were joined to the column plates by CJP welds. In contrast to a W-shape column, forces in the box column are transmitted through the CJP welds of the continuity plates and the PJP welds of the column plates. Thus, it is possible for a weld to fracture if the applied stress is high while the fracture toughness of the weld metal is low.

Figure 12 shows the distribution of maximum principal stress vectors in the box column of Model SOL-EC01 at 2-percent story drift. Most of flange forces are transmitted through the CJP welds joining the continuity plate and the column flange. The transmitted forces are distributed along the depth of the column side plates.

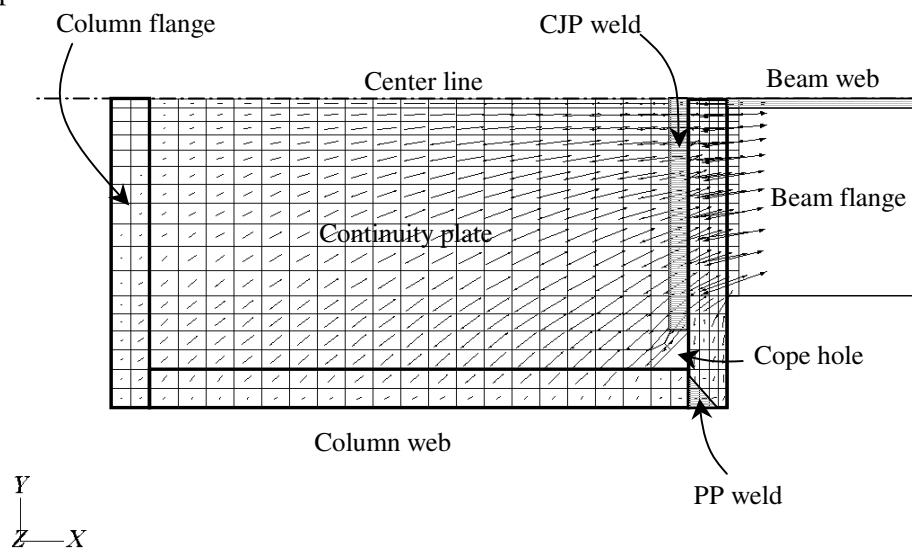


Figure 12. Maximum principal stress vectors in the continuity plate of Model SOL-EC01

CONCLUSIONS

Seismic performance of US Steel box column connections composed of W-shape beams and built-up box-shape columns were investigated from full-scale experimental studies and finite element analyses. All the test specimens were fabricated using pre-Northridge details. Finite element analyses were conducted to investigate the stress and strain distributions of the test specimens at fracture. Based on these studies, the key conclusions can be drawn as follows:

1. The tested pre-Northridge US steel box column connections did not exhibit any plastic rotation in either the beam or the panel zone. The story drift angles associated with beam flange fracture were substantially less than 1-percent. Fracture of beam top flange can precede bottom flange fracture.
2. The peak residual strength of the box column connections following fracture of both beam flanges ranged between 22-percent and 42-percent of the plastic moment of the beam section. The residual strength degraded with repeated cycling. The story drift angle at which the residual strength of the connection was completely lost ranged between 3 and 4 percent. Loss of residual strength in these connections was associated with fracture of the shear tab.
3. In the box column connections, the axial strains across the width of the beam flange near the column were highest at the edges of the beam flange and lowest in the middle of the beam flange. The axial

strain distributions were affected by the out-of-plane stiffness of the column flange plate. As the stiffness increased, the axial strain distribution became uniform.

4. Maximum principal stresses on the beam flange at fracture were much higher than the yield strength of the beam flange. Local yielding of the beam flange can delay the brittle crack propagation while residual stresses induced by welding may increase the propensity to fracture.
5. Flange forces were transmitted to the box column through the CJP welds of the continuity plates and PJP welds of the column plates. Thus, high notch-tough weld metal and careful detailing should be used for such welds to prevent brittle fracture inside the box column.

ACKNOWLEDGMENTS

The study presented in this paper was funded by California Department of Transportation (CALTRANS) through Project 04A1416 "Performance Evaluation of Steel Moment Frames", supervised by Dr. Fadel Alameddine. The findings and opinions presented herein are those of the authors only and may not be shared by the sponsor.

REFERENCES

1. FEMA. "Recommended design criteria for new steel moment frame buildings." FEMA Report No. 350, Washington, D.C.: Federal Emergency Management Agency, 2000.
2. Kim T. "Experimental and analytical performance evaluation of welded steel moment connections to box or deep W-shape columns." Ph.D. Dissertation, Berkeley, CA.: University of California at Berkeley, 2003
3. Whittaker AS, Gilani ASJ, Takhirov SM, and Ostertag C. "Forensic studies of a large cover-plate steel moment-resisting connection." *The Structural Design of Tall Buildings* 2002; 11(4): 265-283
4. SAC. "Protocol for fabrication, inspection, testing, and documentation of beam-column connection tests and other experimental specimens." Report No. SAC/BD-97/02, Sacramento, CA.: SAC Joint Venture, 2000.
5. HKS. "ABAQUS/User's manual and theory manual. Ver. 6.3." Pawtucket, RI.: Hibbit, Karlsson, and Sorenson, 2002.
6. Kim T., Whittaker AS, Gilani ASJ, Bertero VV, and Takhirov SM. "Cover-plate and flange-plate steel moment-resisting connections." *Journal of Structural Engineering*, 2002; 128(4): 474-482.
7. Stojadinovic B, Goel SC, Lee K-H, Margarian AG, and Choi J-H. "Parametric tests on unreinforced steel moment connections." *Journal of Structural Engineering*, 2000; 126(1): 40-49.
8. Zhang J, Dong P. "Residual stresses in welded moment frames and implications for structural performance." *Journal of Structural Engineering*, 2000; 126(3): 306-315.